Superior T memory stem cell persistence supports long-lived T cell memory

Enrico Lugli,[1,2] Maria H. Dominguez,[1] Luca Gattinoni,[3,4] Pratip K. Chattopadhyay,[1] Diane L. Bolton,[1] Kaimei Song,[1] Nichole R. Klatt,[5] Jason M. Brenchley,[5] Monica Vaccari,[6] Emma Gostick,[7] David A. Price,[7] Thomas A. Waldmann,[8] Nicholas P. Restifo,[3] Genoveffa Franchini,[6] and Mario Roederer[1]

[1]ImmunoTechnology Section, Vaccine Research Center (VRC), National Institute of Allergy and Infectious Diseases (NIAID), NIH, Bethesda, Maryland, USA. [2]Unit of Clinical and Experimental Immunology, Humanitas Clinical and Research Center, Rozzano, Italy. [3]Center for Cancer Research, National Cancer Institute (NCI), [4]Experimental Transplantation and Immunology Branch, NCI, [5]Laboratory of Molecular Microbiology, NIAID, and [6]Animal Models and Retroviral Vaccines Section, NCI, NIH, Bethesda, Maryland, USA. [7]Institute of Infection and Immunity, Cardiff University School of Medicine, Cardiff, United Kingdom. [8]Metabolism Branch, NCI, NIH, Bethesda, Maryland, USA.

Long-lived memory T cells are able to persist in the host in the absence of antigen; however, the mechanism by which they are maintained is not well understood. Recently, a subset of human T cells, stem cell memory T cells (T_{SCM} cells), was shown to be self-renewing and multipotent, thereby providing a potential reservoir for T cell memory throughout life. However, their in vivo dynamics and homeostasis still remain to be defined due to the lack of suitable animal models. We identified T cells with a T_{SCM} phenotype and stem cell–like properties in nonhuman primates. These cells were the least-differentiated memory subset, were functionally distinct from conventional memory cells, and served as precursors of central memory. Antigen-specific T_{SCM} cells preferentially localized to LNs and were virtually absent from mucosal surfaces. They were generated in the acute phase of viral infection, preferentially survived in comparison with all other memory cells following elimination of antigen, and stably persisted for the long term. Thus, one mechanism for maintenance of long-term T cell memory derives from the unique homeostatic properties of T_{SCM} cells. Vaccination strategies designed to elicit durable cellular immunity should target the generation of T_{SCM} cells.

Introduction

Long-lived memory T cells are able to persist in the host in the absence of antigen (1). In mice, lymphocytic choriomeningitis virus–specific $CD8^+$ T cells are maintained for life after the acute infection (2). Similarly, in humans, vaccinia virus–specific T cells can be found for many decades after vaccination (3). However, it is unclear whether these memory cells are long lived per se, or differentiate regularly from a rarer, long-lived antigen-specific precursor population undergoing slow homeostatic turnover (4).

Dozens of subsets form the memory T cell compartment (5). Conventionally, antigen-experienced T cells have been divided into central memory (T_{CM}) cells and effector memory (T_{EM}) cells, according to their phenotype, function, differentiation history, and anatomical localization (6). Previously, T_{CM} cells as a whole were thought to exhibit stem cell–like behavior, given their capacity to self-renew and to generate more differentiated progeny in response to multiple stimuli (7). However, this concept was recently challenged by the discovery of an earlier stage of memory T cell differentiation in humans, termed T stem cell memory (T_{SCM}) (8). T_{SCM} cells are precursors of other memory cells including T_{CM} cells, and display enhanced self-renewal capacity; T_{SCM} cells can also generate multiple subsets of memory cells in vitro, and, despite sharing multiple functional attributes with conventional memory cells, they maintain a largely naive-like phenotype, with a core of expressed genes characteristic of naive cells (8). To date, mouse T_{SCM} cells have been described (9, 10), but those specific for viral or tumor antigens have not been identified, making their relevance in physiology and pathology elusive. To address these questions in a relevant animal model, we attempted to characterize T_{SCM} cells (either as a bulk population or antigen-specific) in healthy nonhuman primates (NHPs) and during the course of SIV infection. The identification of such a population in the NHPs, the most widely used animal model for HIV infection, is directly relevant to the design of an effective HIV vaccine.

Results and Discussion

Human $CD8^+$ T_{SCM} cells display a largely naive-like phenotype, but express high levels of CD95, CXCR3, CD122, and LFA-1 (8, 11). In order to characterize the role of T_{SCM} cells in the generation of T cell memory in vivo, we sought to determine whether a similar subset of cells exists in NHPs. In both healthy rhesus macaques (RMs) and pigtail macaques (PTMs), we identified $CD95^{hi}$ $CD8^+$ T cells in the $CD45RA^+CCR7^+CD27^+CD28^+IL\text{-}7R\alpha^+$ naive-like compartment (Figure 1A). Similarly to those in humans, NHP T_{SCM} cells constitute about 2%–3% of circulating $CD8^+$ T cells (Figure 1B). We also identified a $CD4^+$ T_{SCM} subset in PBMCs, with a phenotype and frequency similar to $CD8^+$ T_{SCM} cells (Supplemental Figure 1, A and B; supplemental material available online with this article; doi:10.1172/JCI66327DS1). The NHP model allows a detailed examination of cellular distributions in tissues; we found that $CD8^+$ T_{SCM} cells from healthy RMs are most abundant in LNs, less so in the spleen and bone marrow, and are virtually absent at mucosal surfaces, i.e., the jejunum, the rectum, and the BAL, where only T_{CM} and T_{EM} cells are present (Figure 1C). $CD4^+$ T_{SCM} cells displayed a similar distribution in the body, although less skewed toward the LNs (Supplemental Figure 1C). Thus, T_{SCM} cells have a tropism for secondary lymphoid tissues, with a distribution most similar to naive T (T_N) cells.

Conflict of interest: The authors have declared that no conflict of interest exists.
Citation for this article: *J Clin Invest.* 2013;123(2):594–599. doi:10.1172/JCI66327.

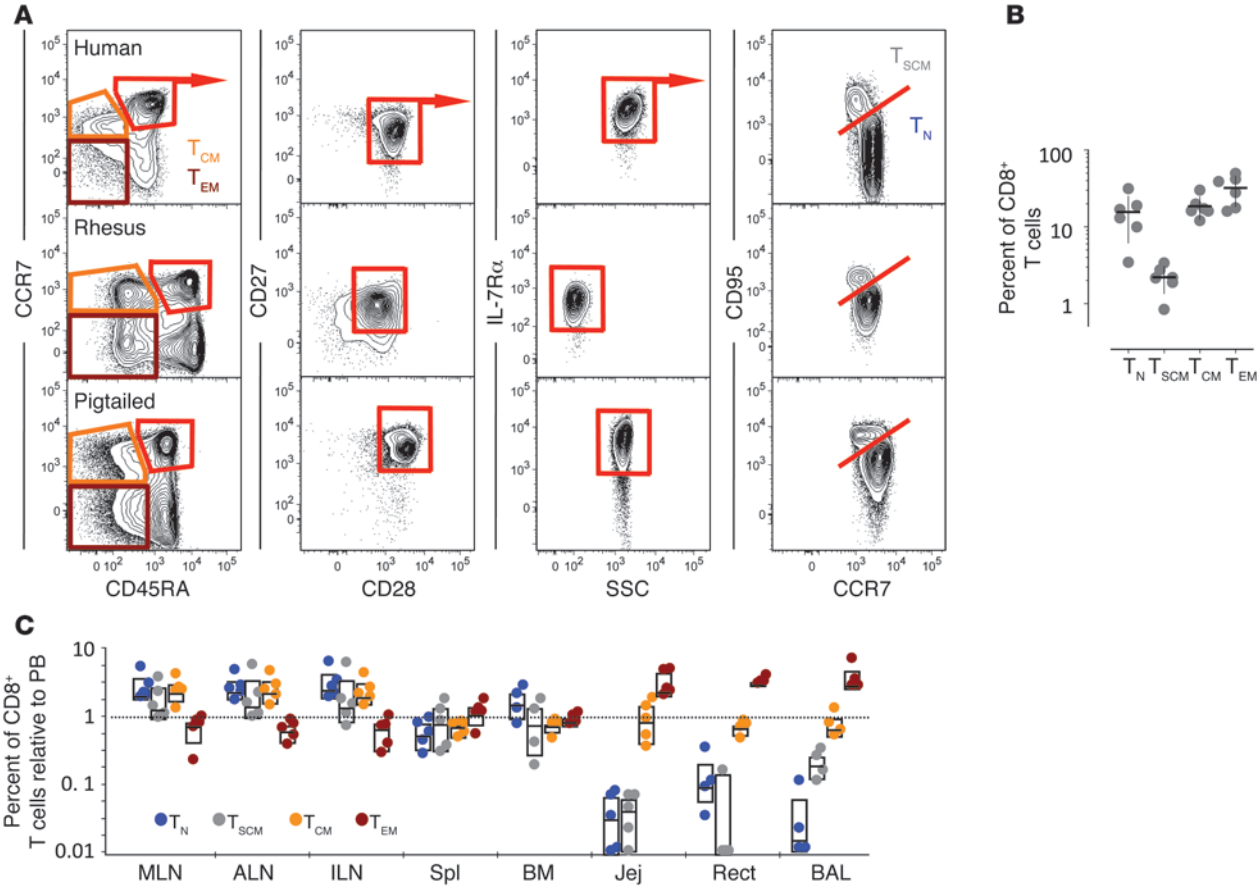

Figure 1
Identification of CD8+ T_{SCM} cells in healthy macaques. (**A**) Flow cytometric analysis of PBMCs from a healthy human donor, an RM, and a PTM. Plots show live CD3+CD8+CD4− lymphocytes. (**B**) Mean ± SEM percentage of CD8+ T_N, T_{SCM}, T_{CM}, and T_{EM} cells in the peripheral blood (PB) of RMs (n = 6). (**C**) As in **B**, but in different organs. Data indicate the proportion relative to PB (dashed bar). Data in **B** and **C** are expressed in log scale. MLN, mesenteric LN; ALN, axillary LN; ILN, inguinal LN; Spl, spleen; Jej, jejunum; Rect, rectum.

We next investigated whether NHP T_{SCM} cells have features of memory cells and precede T_{CM} and T_{EM} cells in terms of differentiation. Immunophenotypic analysis of activation and memory markers (8) indicated that NHP CD8+ T_{SCM} cells from healthy RMs are a discrete subset (Figure 2, A and B). Indeed, they are intermediate between T_N and T_{CM} cells, according to the expression of proteins that are progressively upregulated (CCR5, IL-18Rα) or downregulated (CD38, CD130) with differentiation (Figure 2B). The human T_{SCM} core phenotypic markers CXCR3, CD122 (Figure 2, A and B), and LFA-1 (Supplemental Figure 2, A and B) were also upregulated in T_{SCM} cells compared with T_N cells. Unexpectedly, a relatively large proportion of T_{SCM} cells were proliferating (Ki-67+) in the PBMCs (Figure 2A), but not in the LNs, spleen, or BM (Supplemental Figure 2C). In all sites, T_{SCM} cells were mostly HLA-DR negative. Similar phenotypic data were obtained for CD4+ T_{SCM} cells (Supplemental Figure 1D).

To assess the cytokine production capability of NHP T_{SCM} cells, we stimulated PBMCs from healthy RMs with staphylococcal enterotoxin B (SEB). Following stimulation, all subsets of memory T cells produced IFN-γ, TNF, and IL-2 (Figure 2C). The patterns of cytokine expression show that T_{SCM} cells differ from T_{CM} and T_{EM} cells, with a decreased proportion of cells producing a combination of IL-2 and TNF, but not IFN-γ, and an increased proportion of cells producing IFN-γ and IL-2 or IFN-γ only. Overall, their quality of cytokine production differed from conventional memory T cells (Figure 2C). T_{SCM} cells also display attributes of memory in vivo, as proliferating (Ki-67+) T_{SCM} cells incorporated BrdU following $SIV_{mac}239$ infection in PTMs similarly to conventional T_{CM} and T_{EM} cells (Supplemental Figure 2D). In contrast, BrdU incorporation by T_N cells was negligible.

To further assess whether T_{SCM} cells from healthy RMs constitute discrete, less-differentiated memory cells, we evaluated their multipotency (i.e., to generate other subsets) and self-renewing capability (i.e., to maintain a T_{SCM} phenotype) in response to TCR stimulation in vitro with αCD3/CD28 antibodies (Figure 2D). In the proliferating (CFSE-diluted) fraction, T_{SCM} phenotype cells could only be recovered from sort-purified T_N or T_{SCM} cells. In addition, T_{SCM} cells were also able to generate cells with a T_{CM}, T_{EM}, and terminal effector T (T_{TE}) phenotype (Figure 2D). Importantly, T_{CM} cells could not generate T_{SCM} cells, but did generate T_{CM} and T_{EM} cells. Together, these data indicate that T_{SCM} cells constitute a discrete memory subset and support the concept that T_{SCM} cells serve as precursors of other memory cells, according to the relationship $T_{SCM} \rightarrow T_{CM} \rightarrow T_{EM} \rightarrow T_{TE}$.

To determine the dynamics of antigen-specific T cell subsets during a natural infection in vivo, we enumerated SIV-specific CD8+ T cells in RMs using Mamu-A*01 pMHCI multimers

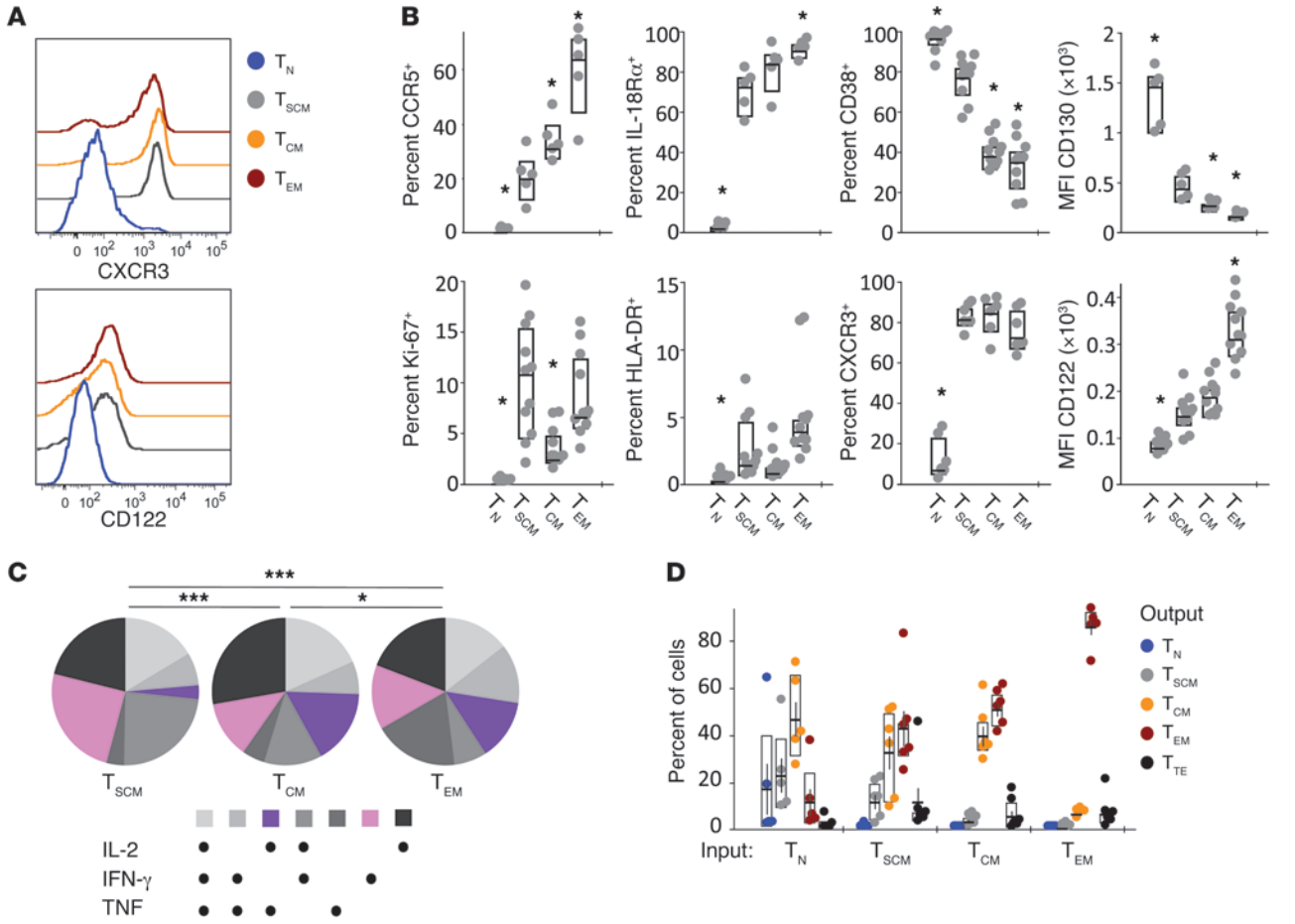

Figure 2

T_{SCM} cells from healthy RMs are phenotypically and functionally distinct T cells. (**A**) Expression of CXCR3 and CD122 on CD8$^+$ T_N, T_{SCM}, T_{CM}, and T_{EM} cells by flow cytometry. (**B**) Percentage of CD8$^+$ T cell subsets expressing CCR5, IL-18Rα, CD38, Ki-67, HLA-DR, or CXCR3. CD130 and CD122 are indicated as MFI. *$P < 0.05$ versus T_{SCM}. (**C**) Pie charts representing the proportion of cells producing different combinations of IL-2, IFN-γ, and TNF after SEB stimulation. *$P < 0.05$, ***$P < 0.001$. (**D**) Mean percentage of cells with various differentiation phenotypes recovered following activation of FACS-sorted T_N, T_{SCM}, T_{CM}, and T_{EM} cells by αCD3/CD28 antibodies in vitro for 5 days ($n = 6$). The analysis was carried out on cells that diluted CFSE. Boxes in **B** and **D** show interquartile range and median values.

presenting SIV-derived Gag CM9 or Tat-TL8 peptides (Supplemental Figure 3A). Antigen-specific T_{SCM} cells were detected within both CM9- and TL8-specific cells at day 21 after infection, thus demonstrating that they are elicited early (Figure 3A). The antigen-specific T_{SCM} cells were not merely "bystander" cells, but displayed evidence of activation (HLA-DR$^+$, CD38^{bright}) and proliferation (Ki-67$^+$) (Supplemental Figure 3B). At day 21 after infection, CM9- and TL8-specific CD8$^+$ T cells were dominated by T_{EM}-like cells, while T_{SCM}, T_{CM}, and T_{TE} cells constituted a small proportion of the total response (Figure 3, A and B).

The biology of the CM9 and TL8 Mamu-A*01–restricted epitopes is highly divergent. Unlike CM9, which is generally maintained intact throughout the chronic phase of infection, the TL8 uniformly undergoes escape mutation within 4–5 weeks after $SIV_{mac}239$ or $SIV_{mac}251$ infection in 100% of animals (12–14). Tat-TL8 sequence variants do not stimulate TL8-specific T cells due to their reduced capability to bind the pMamu-A*01 class I molecule (12) or to signal through the TCR (14). Following TL8 escape, there is at least a 10^5-fold decrease in the relative antigen load of TL8 versus CM9. Using this model, it is thus possible to investigate the relative antigen dependence of the different T cell subsets. As expected, viral escape from TL8-directed CTLs resulted in a dramatic decrease in the frequency of total circulating TL8-specific CD8$^+$ T cells between days 21 and 70–120 after infection (Supplemental Figure 3C). Conversely, CM9-specific CD8$^+$ T cells were maintained at high levels throughout the course of the infection (Supplemental Figure 3C). Notably, despite the near-complete elimination of antigen (extremely low levels from residual "archival," unmutated virus may persist) (12), TL8-specific CD8$^+$ T cells did not disappear, but remained detectable beyond day 335 after infection (Supplemental Figure 3C).

Phenotypic analysis of the TL8-specific population revealed a significant difference in the dynamics of memory subsets in response to viral escape mutation. Indeed, the proportion of TL8-specific T_{EM} cells decreased dramatically in favor of the less differentiated T_{SCM} and T_{CM} cells (Figure 3, A and B). By day 70 after infection, T_{SCM} cells constituted approximately 25% of the total TL8-specific response (Figure 3B). In contrast, memory subset distribution within the CM9-specific CD8$^+$ T cells remained unchanged between days 21 and 70 after infection

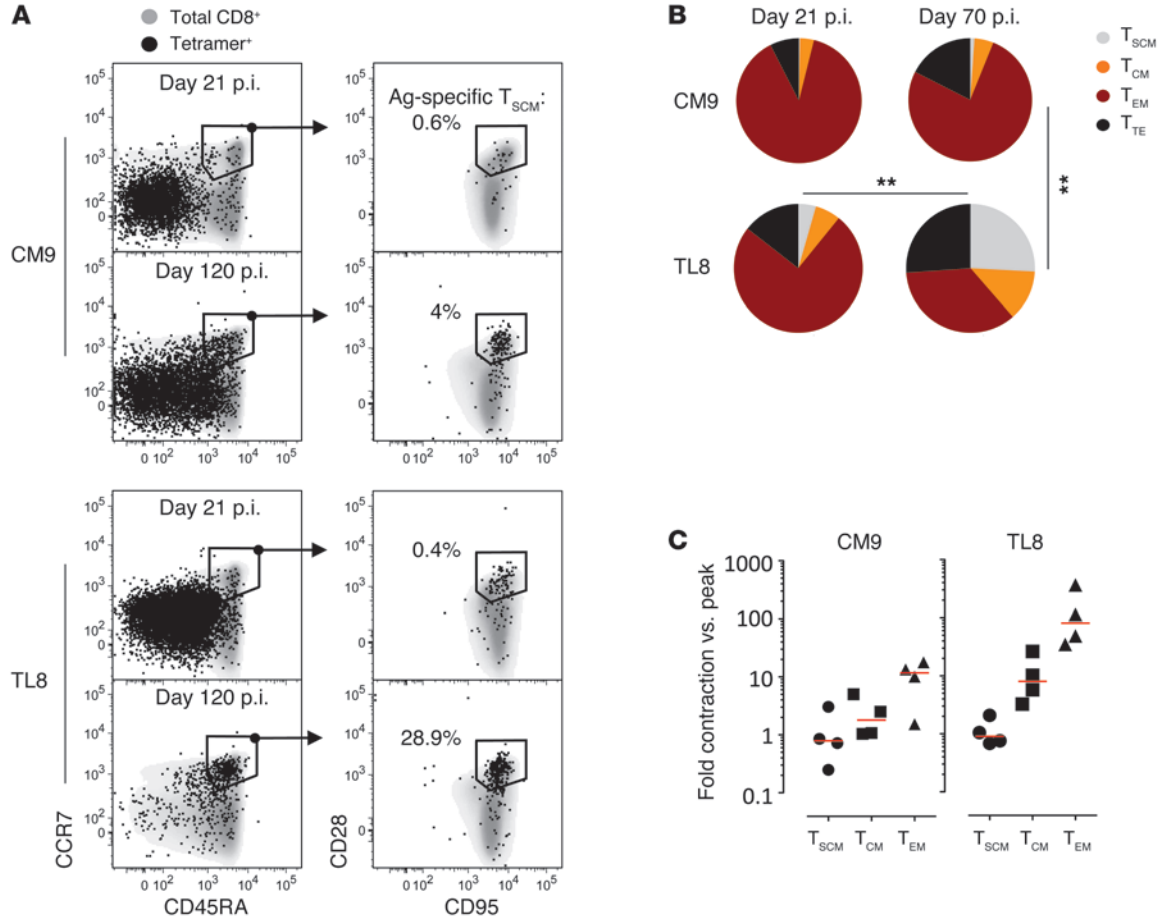

Figure 3

Preferential maintenance of T_{SCM} cells following escape of the cognate antigen. (**A**) Tetramer$^+$CD8$^+$ T cells (black) superimposed on total CD8$^+$ T cells (gray) at day 21 and day 120 after infection with $SIV_{mac}251$. Gates first identify CD45RA$^+$CCR7$^+$ cells, then CD28$^+$CD95$^+$ T_{SCM} cells. Numbers in the CD28 versus CD95 plots indicate the percentage of T_{SCM} cells out of total antigen-specific (tetramer$^+$) T cells. (**B**) Pie charts depicting the proportion of CM9- and TL8-specific CD8$^+$ T cells with different phenotypes (T_{SCM}: CD45RA$^+$CCR7$^+$CD28$^+$CD95$^+$; T_{CM}: CD45RA$^-$CCR7$^+$; T_{EM}: CD45RA$^-$CCR7$^-$; T_{TE}: CD45RA$^+$CCR7$^-$) at day 21 and day 70 after infection ($n = 6$). $^{**}P < 0.01$. (**C**) Fold change in the absolute count of SIV-specific CD8$^+$ T cells between day 21 and day 70 after infection ($n = 4$). Red bars indicate median values. Data are expressed in log scale. p.i., post infection.

(Figure 3B). Furthermore, as would be expected from a loss of antigen, TL8-specific, but not CM9-specific T_{SCM} and T_{CM} cells, became quiescent (Ki-67$^-$, HLA-DR$^-$) at day 70 after infection (Supplemental Figure 3B).

Following antigen loss, TL8-specific T_{CM} and T_{EM} cells underwent considerable attrition (respectively, ~10- and ~100-fold decrease in the absolute count at day 70 versus day 14), while T_{SCM} cells did not (Figure 3C and Supplemental Figure 3D). Similarly, CM9-specific T_{SCM} counts did not change over time, while the CM9-specific T_{CM} and T_{EM} cells contracted, albeit at markedly slower rates compared with TL8-specific CD8$^+$ T cells (Supplemental Figure 3D), reflecting the 1-log decrease in viral load following peak viremia by day 70 after infection (i.e., establishment of the viral set point).

CM9- and TL8-specific subsets, FACS-sorted from a chronically SIV-infected RM, were fully functional as they proliferated following cognate peptide stimulation in vitro (Supplemental Figure 4A). Importantly, each T cell subset regenerated cells with the same phenotype and simultaneously derived more, not less, differentiated progeny according to the relationship $T_{SCM} \rightarrow T_{CM} \rightarrow T_{EM}$ (Supplemental Figure 4B), thus recapitulating the results depicted in Figure 2D and further demonstrating the multipotency and self-renewing capability of T_{SCM} cells in vitro. The distribution of memory subsets observed at day 70 after infection within both the CM9- and TL8-specific populations was similar in 4 animals at more than 335 days after infection (Supplemental Figure 5A).

Following escape mutation of the TL8 epitope, the frequency of SIV-specific T cell subsets did not change in the inguinal LNs over time in 2 animals, suggesting that their lymphoid localization is not time dependent (Supplemental Figure 5B). Moreover, the same cells maintained a stable pattern of localization, as described in Figure 1C, during late chronic infection (Supplemental Figure 5C). Collectively, these findings indicate that T_{SCM} cells are stable, long-lived memory cells with enhanced survival capacity compared with conventional memory cells when little or no antigen is present.

Freshly isolated CM9-specific T_{SCM} cells were indeed less proapoptotic in vitro than T_{CM} and T_{EM} cells during chronic infection (Supplemental Figure 6, A and B). Similarly, fewer TL8-specific T_{SCM} cells

bound annexin V compared with the total memory fraction (there were insufficient T cells for evaluation of TL8-specific T_{CM} and T_{EM} cells individually; Supplemental Figure 6B). Consistent with the lack of chronic antigen exposure, TL8-specific cells were less proapoptotic than CM9-specific cells (Supplemental Figure 6B).

We thus reasoned that the preferential expression of antiapoptotic molecules in T_{SCM} cells could be associated with their preferential survival. We could not quantify gene expression in antigen-specific cells due to their paucity. Instead, we sorted "resting" versus "blasting" (presumably antigen-responding) $CD8^+$ T cell subsets according to their scatter properties (Supplemental Figure 7A). The "blasting" lymphocytes uniformly expressed high levels of HLA-DR, indicative of activation in vivo (Supplemental Figure 7B). Notably, genes such as *LEF1* (regulating self-renewal), *BCL2,* and *MCL1* (both antiapoptotic) were not differentially expressed among "resting" memory subsets, but were specifically upregulated to high levels in "blasting" T_{SCM} cells (Supplemental Figure 7C).

In summary, our data show that NHP T_{SCM} cells are closely related to human T_{SCM} cells, and constitute a discrete memory T cell subset, distinct from T_{CM} cells, on the basis of: (a) surface immunophenotype, (b) localization in the body, (c) cytokine production, and (d) in vivo turnover. Although T_{CM} cells were demonstrated to possess stem cell–like properties in multiple experimental conditions (7), our data suggest that T_{SCM} cells are superior to T_{CM} cells in this regard owing to their superior self-renewing capability and multipotency, their relative antigen dependence in vivo, and their apoptotic refractoriness. Notably, these properties are not unique to T_{SCM} cells, but rather are highly preferentially associated with the T_{SCM} subset. And importantly, the superior persistence of T_{SCM} cells following antigen loss suggests that they are the main precursors of T cell memory in the postantigen phase.

Maintenance of antigen-specific T_{SCM} cells is likely intrinsically programmed. We exclude the possibility that the T_{SCM} pool is maintained by the continuous recruitment of newly generated naive T cells by thymic output (15) in our model, as thymic output is severely impaired in chronic, untreated HIV and SIV infections (16, 17). In addition, we find equivalent maintenance of CM9- and TL8-specific T_{SCM} cells despite a profound difference in antigen availability.

Our data strongly suggest that T_{SCM} cells play a crucial role in supporting long-term cellular immunity in vivo. Future studies aimed at identifying antigen-specific T_{SCM} cells in adoptive transfer models are required to define whether they are uniquely suited for this function. On the basis of these properties, we propose that future vaccination strategies designed to generate durable immunity should target the induction of T_{SCM} cells. Nevertheless, cellular immunotherapy strategies will need to exploit T_{SCM} properties to support the persistence of in vivo–transferred virus- and tumor-specific T cells.

Methods

Animals. Animals were handled in accordance with the standards of the American Association for the Accreditation of Laboratory Animal Care (AAALAC) and meet NIH standards (*Guide for the Care and Use of Laboratory Animals*. NIH publication no. 85-23. Revised 1985). See Supplemental Methods for animal procedures.

*Antibodies, Mamu-A*01 tetramers, and flow cytometry*. Surface and intracellular analysis of protein expression and cytokine production was performed as described (8, 18). Tetramer staining was conducted at 37°C for 10 minutes. Cells were analyzed and sorted using a modified LSR II and FACSAria II, respectively (BD Biosciences).

Apoptosis studies. Fresh PBMCs were cultured in complete RPMI 1640 medium supplemented with αCD49d and αCD28 antibodies (both at 1 μg/ml; BD Biosciences) at 37°C for 42 hours. Surface phosphatidylserine expression was revealed as described (18).

Proliferation studies. Cell proliferation was determined by dilution of CFSE (Life Technologies) as described (8). Labeled cells were stimulated for 6 days with 2 μg/ml CM9 and TL8 peptides in the presence of sorted, $CD3^-$ autologous antigen-presenting cells (1:1 ratio to T cells) or with plate-bound αCD3 (10 μg/ml; clone FN18) plus soluble αCD28 (1 μg/ml; clone CD28.2) antibodies.

In vivo BrdU labeling. Administration of BrdU (Sigma-Aldrich) and analysis of its incorporation were performed as described (18).

Gene expression analysis. $CD8^+$ T cell subsets were sorted as depicted in Supplemental Figure 7. See Supplemental Methods for gene expression quantification procedures.

Statistics. Analyses were performed using Prism (GraphPad Software Inc.), JMP (SAS Institute Inc.), and SPICE (NIAID, NIH) (19). Nonparametric Wilcoxon rank tests were used to compare distributions. When possible, a paired Student's *t* test (2 tailed) was used. In some cases, nonparametric 1-way ANOVA (Kruskal-Wallis test) was used to compare 3 or more groups. Distributions shown with pie charts were compared with SPICE. *P* values were considered significant when less than 0.05.

Study approval. All animal procedures were reviewed and approved by the Institutional Animal Care and Usage Committee of the VRC, the NIAID, the NCI, and Oregon Health and Science University (Portland, Oregon, USA). The anonymous human blood sample (Figure 1A) was obtained from the NIH blood bank under institutional review board exemption.

Acknowledgments

We thank Joanne Yu for antibody conjugation; the VRC Flow Cytometry Core for cell sorting; Richard Koup, Constantinos Petrovas, Takuya Yamamoto, Louis Picker, and Andrew Sylwester for sharing MamuA*01 samples; the VRC NHP Immunogenicity Core for sample processing; and Daniel Douek for critical discussion. This research was supported by the NIAID and NCI Intramural Research Programs at the NIH.

Received for publication August 13, 2012, and accepted in revised form November 1, 2012.

Address correspondence to: Enrico Lugli or Mario Roederer, ImmunoTechnology Section, Vaccine Research Center, NIAID, NIH, 40, Convent Dr., Bethesda, Maryland 20892, USA. Phone: 301.594.8491; Fax: 301.480.2788; E-mail: luglie@mail.nih.gov (E. Lugli). E-mail: roederer@nih.gov (M. Roederer).

1. Zinkernagel RM, Bachmann MF, Kundig TM, Oehen S, Pirchet H, Hengartner H. On immunological memory. *Annu Rev Immunol.* 1996;14:333–367.
2. Murali-Krishna K, et al. Counting antigen-specific CD8 T cells: a reevaluation of bystander activation during viral infection. *Immunity*. 1998; 8(2):177–187.
3. Hammarlund E, et al. Duration of antiviral immunity after smallpox vaccination. *Nat Med*. 2003; 9(9):1131–1137.
4. Surh CD, Sprent J. Homeostasis of naive and memory T cells. *Immunity*. 2008;29(6):848–862.
5. Perfetto SP, Chattopadhyay PK, Roederer M. Seventeen-colour flow cytometry: unravelling the immune system. *Nat Rev Immunol*. 2004; 4(8):648–655.
6. Sallusto F, Geginat J, Lanzavecchia A. Central memory and effector memory T cell subsets: function, generation, and maintenance. *Annu Rev Immunol.* 2004;22:745–763.
7. Stemberger C, Neuenhahn M, Gebhardt FE, Schiemann M, Buchholz VR, Busch DH. Stem cell-like plasticity of naive and distinct memory $CD8^+$ T cell subsets. *Semin Immunol*. 2009;21(2):62–68.

8. Gattinoni L, et al. A human memory T cell subset with stem cell-like properties. *Nat Med*. 2011; 17(10):1290–1297.
9. Gattinoni L, et al. Wnt signaling arrests effector T cell differentiation and generates $CD8^+$ memory stem cells. *Nat Med*. 2009;15(7):808–813.
10. Zhang Y, Joe G, Hexner E, Zhu J, Emerson SG. Host-reactive $CD8^+$ memory stem cells in graft-versus-host disease. *Nat Med*. 2005;11(12):1299–1305.
11. Lugli E, et al. Identification, isolation and in vitro expansion of human and nonhuman primate T stem cell memory cells. *Nat Protoc*. 2012;8(1):33–42.
12. Allen TM, et al. Tat-specific cytotoxic T lymphocytes select for SIV escape variants during resolution of primary viraemia. *Nature*. 2000; 407(6802):386–390.
13. O'Connor DH, et al. Acute phase cytotoxic T lymphocyte escape is a hallmark of simian immunodeficiency virus infection. *Nat Med*. 2002; 8(5):493–499.
14. Price DA, et al. T cell receptor recognition motifs govern immune escape patterns in acute SIV infection. *Immunity*. 2004;21(6):793–803.
15. Vezys V, et al. Continuous recruitment of naive T cells contributes to heterogeneity of antiviral CD8 T cells during persistent infection. *J Exp Med*. 2006; 203(10):2263–2269.
16. Douek DC, Picker LJ, Koup RA. T cell dynamics in HIV-1 infection. *Annu Rev Immunol*. 2003; 21:265–304.
17. Richardson MW, et al. T-cell receptor excision circles (TREC) in SHIV 89.6p and SIVmac251 models of HIV-1 infection. *DNA Cell Biol*. 2004;23(1):1–13.
18. Lugli E, Mueller YM, Lewis MG, Villinger F, Katsikis PD, Roederer M. IL-15 delays suppression and fails to promote immune reconstitution in virally suppressed chronically SIV-infected macaques. *Blood*. 2011;118(9):2520–2529.
19. Roederer M, Nozzi JL, Nason MX. SPICE: Exploration and analysis of post-cytometric complex multivariate datasets. *Cytometry A*. 2011; 79(2):167–174.